Percutaneous Microwave Ablation with a Long Side-Firing Antenna Array Can Successfully Treat a Nonsurgical Chronic Ovine Atrial Flutter Model

TOON WEI LIM, M.B.B.S., F.R.A.C.P.,*,† RAY CLOUT,‡ MICHAEL A. BARRY, B.Sc.,† JUNTANG LU,† KAIMIN HUANG, B.Sc.(Hons),† and STUART P. THOMAS, B.Med., Ph.D., F.R.A.C.P.*,†

From the *University of Sydney, Sydney, Australia; †Department of Cardiology, Westmead Hospital, Sydney, Australia; and ‡University of Technology, Sydney, Australia

Microwave Ablation of an Ovine Atrial Flutter Model. ***Introduction:*** **Long side-firing microwave (MW) arrays can deliver energy uniformly over its length without the need for intimate endocardial contact. We hypothesize that a novel 6 Fr 20 mm long percutaneous high-efficiency MW antenna array ablation catheter can rapidly create long, continuous, and transmural linear ablation lesions.**

Methods and Results: **Cavotricuspid isthmus (CTI)-dependent atrial flutter (AFL) was created in 11 sheep by a line of radiofrequency ablation lesions in the posterior right atrium (RA) linking the venae cavae. After 4–6 weeks recovery, CTI-dependent AFL was still inducible in all 11 sheep (cycle length 178 ± 13 ms). MW ablation of the CTI at 100 W for 30 seconds was then performed with an endpoint of AFL noninducibility. AFL was not inducible in all 11 sheep after 4.3 ± 3.3 MW applications (129 ± 99 seconds). The last 6 animals needed fewer ablations (2.2 ± 1.5) and 3 of these sheep required only a single ablation. Although conduction times from proximal coronary sinus to lateral RA and vice versa increased postablation (51 ± 14 ms to 118 ± 31 ms [P = 0.0002] and 60 ± 13 ms to 119 ± 28 ms [P = 0.0001], respectively), AFL was still inducible in 2 sheep and further ablation was needed to reach the endpoint.**

Conclusions: **High-efficiency side-firing MW array ablation can rapidly create long linear and electrically intact lesions in an ovine AFL model. AFL noninducibility may be a more reliable indicator than CTI conduction times of an intact line of ablation in this animal model.** *(J Cardiovasc Electrophysiol, Vol. 20, pp. 1255-1261, November 2009)*

microwaves, catheter ablation, atrial flutter, cavotricuspid isthmus

Introduction

Percutaneous transvascular catheter ablation, first employed in the late 1980s,[1] is now the main curative technique for the treatment of cardiac arrhythmias. The most widely used energy source for these procedures is radiofrequency ablation. Radiofrequency energy is safe[2] and is usually effective, but there are some limitations to this technology. To increase lesion depth, higher power ablations are needed.[3,4] However, higher power outputs can cause overheating at the endocardial surface resulting in coagulum formation and embolic complications. This is partly overcome by more recent externally irrigated catheter designs.[5] Nevertheless, it is still dependent on good contact between the electrode and the endocardium[6] and catheter stability for lesion creation, which is particularly problematic when ablating over regions with prominent ridges or depressions like the cavotricuspid isthmus (CTI). Creating continuous linear lesions with a series of spot lesions is also time consuming and technically difficult.

Microwave (MW) ablation catheters have been developed to overcome some of these problems. They have the capacity to generate lesions of greater depth and volume than radiofrequency ablation, and are less dependent on tissue contact.[7] Handheld MW probes have been used in open heart surgery,[8,9] but experience with percutaneous ablation catheters for clinical applications is limited.[10,11]

One of the difficulties with catheter technology development has been the availability of an animal model that will enable us to ablate to an electrophysiological endpoint. Previous MW ablation studies have relied on demonstrating delayed conduction across the CTI as the endpoint for successful ablation rather than the elimination of arrhythmia inducibility.[12,13] An acute canine model of atrial flutter (AFL) was first described by Rosenblueth and Garcia Ramos in 1947.[14] Since then, variations of this model, including chronic AFL models created by incising and resuturing the right atrium (RA) have been developed, but these have all required thoracotomy.[15,16]

The aim of our study was to first develop a chronic ovine AFL model using purely percutaneous techniques and then to use that to test the effectiveness of a novel high-efficiency coaxial ring slot array MW ablation catheter that is designed to create long linear lesions.

This project received funding in the form of a development grant from the National Health and Medical Research Council (Australia).

S. Thomas owns a patent relevant to this topic.

Address for correspondence: Stuart P. Thomas, B.Med., Ph.D., F.R.A.C.P., Department of Cardiology, Westmead Hospital, Cnr Hawkesbury and Darcy Roads, Westmead, NSW 2145, Australia. Fax: 61-2-9845-8323; E-mail: stuartpt@yahoo.com

Manuscript received 24 February 2009; Revised manuscript received 19 May 2009; Accepted for publication 22 May 2009.

doi: 10.1111/j.1540-8167.2009.01545.x

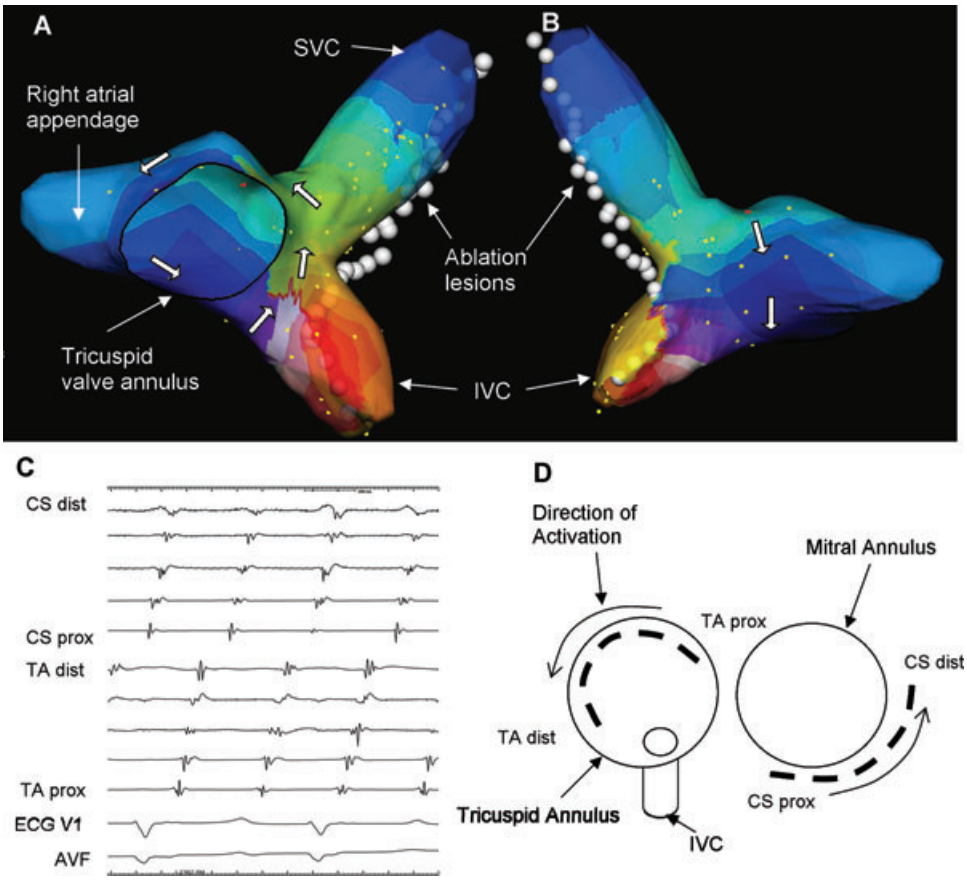

Figure 1. *Right atrial ablation to create atrial flutter (AFL). (A and B) Right atrial anatomy rendered with a 3D electroanatomical system. Panel A is an anteroposterior (ventrodorsal) view, while panel B is a posteroanterior (dorsoventral) view. A line of ablation lesions is marked as white spheres on the posterior right atrium (RA) connecting the superior vena cava (SVC) to the inferior vena cava (IVC). The white arrows indicate the anticlockwise direction of the AFL activation around the tricuspid annulus. (C) Intracardiac electrograms during anticlockwise tricuspid annular flutter showing proximal to distal activation of the tricuspid annulus (TA) catheter that precedes proximal to distal activation the coronary sinus catheter (CS). (D) Schematic diagram of positioning of the decapolar catheters in the RA and CS.*

Methods

Procedure 1: AFL Model Creation

Merino cross wethers were used in this study. The mean weight for the 11 animals in this study was 48.6 ± 4.7 kg. All experiments were performed under general anesthesia induced with intravenous propofol and maintained with isoflurane and mechanical ventilation. A decapolar catheter (Livewire, St. Jude Medical, St. Paul, Minnetonka, MN, USA) was placed in the coronary sinus via the 7 Fr jugular vein sheath, while another was positioned around the tricuspid annulus via a 7 Fr right femoral venous sheath (Fig. 1D). A quadpolar open irrigated radiofrequency ablation catheter (Thermocool, Biosense Webster, Diamond Bar, CA, USA) was placed in the RA through a long deflectable sheath (Agilis NxT, St. Jude Medical) via the right femoral vein. Arterial pressure was monitored during the procedure through a 6 Fr sheath in the left femoral artery.

A 3-dimensional (3D) anatomical rendering of the RA and both venae cavae was acquired using an electroanatomic mapping system (EnSite NavX, St. Jude Medical) and the ablation catheter (Fig. 1A,B). Rapid atrial burst pacing was then performed from the RA and coronary sinus in an attempt to induce AFL. Sheep that had organized atrial tachycardia prior to any ablation were excluded.

If AFL was not inducible, an intercaval line of radiofrequency ablation lesions was created on the posterior RA from the superior vena cava down to the inferior vena cava (Fig. 1A,B). We then attempted to induce AFL again using rapid atrial pacing. If AFL could not be induced, activation mapping during proximal coronary sinus pacing was used to identify gaps in the line of ablation. These were reablated and rapid atrial pacing was performed again. This process was repeated until all gaps in the line were ablated and sustained AFL was inducible. The AFL was mapped using the electroanatomic mapping system.

The sheep were recovered and allowed to recuperate for 6 weeks before the second procedure.

Procedure 2: MW Ablation

The second procedure was similarly performed under general anesthesia with mechanical ventilation, arterial pressure monitoring and guided by a 3D electroanatomical mapping system as described above. A decapolar catheter (Livewire, St. Jude Medical) was placed in the coronary sinus via a jugular venous sheath, and another was positioned in the RA around the tricuspid annulus via a femoral venous

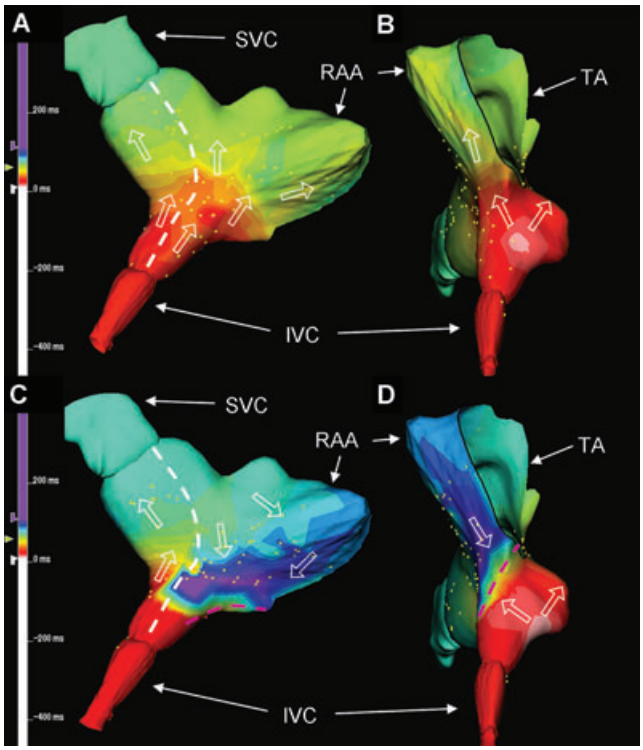

Figure 2. *Propagation maps during proximal coronary sinus pacing before and after microwave (MW) ablation. Activation maps of the right atrium (RA) during proximal coronary sinus pacing is shown in posterior (A, C) and inferior (B, D) views with the direction of activation indicated by open white arrows. Before ablation (A, B), activation begins near the inferior vena cava (IVC) and propagates through the cavotricuspid isthmus (CTI) (B), with caudocranial activation on both sides of the intercaval line (broken white line) ablated at the previous procedure and in the lateral RA. After MW ablation (C,D), a new line of block in the CTI (broken purple line) reverses the direction of activation in the lateral RA while it remains caudocranial medial to the intercaval line. RAA = right atrial appendage; SVC = superior vena cava; TA = tricuspid annulus.*

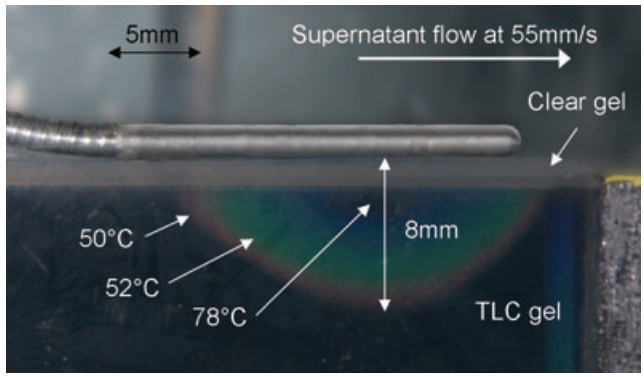

Figure 3. *Microwave (MW) catheter temperature distribution. A MW catheter was positioned over a myocardial phantom gel incorporating thermochromic liquid crystals (TLC) to demonstrate its hyperthermic zone.[25] Normal saline at 37°C flowing at 55 mm/s was used to simulate blood cooling. At 100 W after 30 seconds, the liquid crystals has changed color at predictable temperatures to show zones of hyperthermia as indicated that extend to 8 mm depth underneath the midpoint of the antenna array. Gel boiling point is 90°C,which has not been reached at the catheter—gel interface.*

sheath. Conduction times between the proximal coronary sinus and the low lateral RA in both directions were determined by differential pacing in the baseline state. Activation mapping of the RA was performed during proximal coronary sinus pacing to demonstrate the presence of conduction through the CTI (Fig. 2A). Rapid atrial burst pacing was then performed to induce AFL that was then mapped. This was then terminated by overdrive pacing before MW ablation.

A 20 mm long coaxial ring slot array MW ablation antennae (Fig. 3) was used for performing MW ablation. This antenna has a series of periodic circumferential slots on a coaxial cable appropriately spaced to form slot voltages of equal magnitude in order to create multiple excitation sources.[17] MW energy was generated using a 2.45 GHz MW power generator (ASTeX AX2000, MKS, ASTeX Products, Wilmington, MA, USA). Measurements of delivered, reflected and absorbed power were made with a waveguide impedance analyzer (HOMER, S-TEAM Trading, Bratislava, Slovak Republic) and custom software. The ablation catheter was positioned over the CTI through the deflectable sheath via the right femoral vein. Positioning was guided by fluoroscopy, the electroanatomical mapping system, and local electrograms. Ablations were performed at 100 W for 30 seconds. The first ablation was performed with the MW catheter positioned to just overlie the atrioventricular junction at its distal end (Fig. 4). After the application of MW energy, bidirectional conduction times between the proximal coronary sinus and low lateral RA were remeasured and AFL induction by rapid atrial pacing was performed. The electrophysiological endpoint was noninducibility of AFL and reversal of the activation pattern of the lateral RA during coronary sinus pacing seen as anticlockwise activation of the tricuspid annulus (Fig. 5). If that ablation was not successful, the MW catheter was repositioned before another ablation was performed. This was guided by mapping the CTI region for persisting electrograms along the line of ablation from the tricuspid annulus to inferior vena cava. Bidirectional conduction times and AFL inducibility were rechecked after the ablation. If the endpoint was not reached, then the catheter was repositioned again and the process repeated until the endpoint was reached. When the endpoint was reached, activation mapping of the RA was performed again to confirm conduction block at the CTI (Fig. 2B).

At the conclusion of the experiment, nitro blue tetrazolium was infused to delineate the ablation lesions more clearly before the sheep were sacrificed and the hearts excised for histology.

Statistical Analysis

Continuous variables were expressed as mean ± standard deviation. Analysis was performed using SPSS version 14 (SPSS Inc., Chicago, IL, USA). Independent samples of continuous variables were compared using the Student *t*-test, while paired measurements were compared using paired *t*-tests.

Ethics

This study was performed with the approval and under the supervision of the Westmead Hospital Animal Ethics Committee.

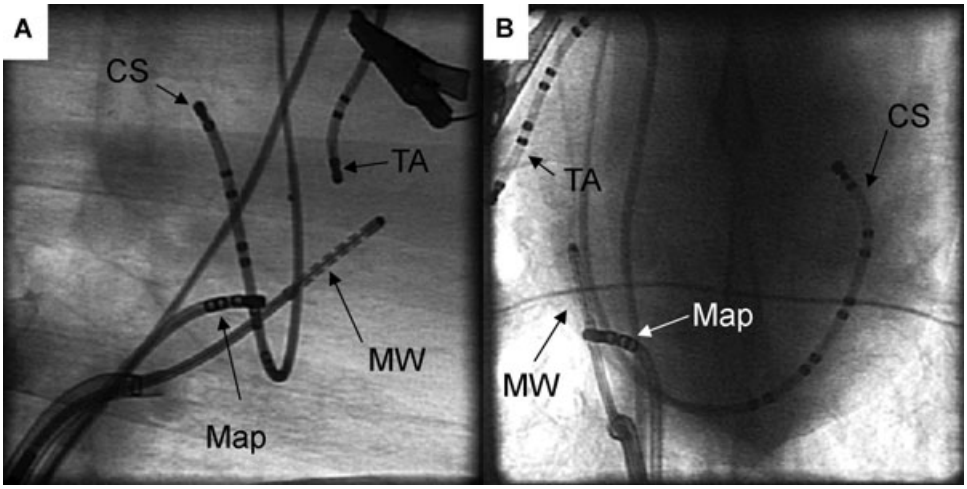

Figure 4. *Fluoroscopic images of microwave (MW) ablation catheter positioning. (A) Right lateral view (approximates right anterior oblique 30° view in humans). The plane of the tricuspid annulus catheter (TA) and coronary sinus catheter (CS) indicates the position of the tricuspid and mitral valves, respectively. The distal tip of the microwave catheter (MW) lies just over the atrioventricular junction. (B) Anteroposterior view (approximates left anterior oblique 55° in humans) of the catheters in the same positions. The mapping catheter (Map) was left in situ to indicate the most posterior part of the isthmus where local electrograms were still detectable. This first ablation did not produce conduction block in the isthmus or make the flutter noninducible. A further ablation with the MW catheter pulled back toward to cover the persisting electrograms more posteriorly resulted in conduction block and rendered the flutter noninducible.*

Results

AFL Model

AFL was inducible in 4 sheep before any ablation and they were excluded. The remaining 11 sheep in this experiment only had nonsustained runs of atrial fibrillation with rapid atrial pacing. After radiofrequency ablation of the posterior right atrial intercaval line, AFL was inducible with rapid atrial pacing in all 11 sheep. The activation pattern in the coronary sinus was proximal to distal in all cases (Fig. 1C). Electroanatomical mapping demonstrated activation of the RA that was either clockwise (n = 9, cycle length 163 ± 17 ms) or anticlockwise (n = 7, cycle length 178 ± 11 ms) around tricuspid annulus. Activation on either side of the ablation line in the posterior RA was always in opposite directions (Fig. 1A,B), that is, caudocranial on one side and craniocaudal on the other depending on whether the AFL was clockwise or anticlockwise. Both anticlockwise and clockwise flutters were inducible in 5 animals.

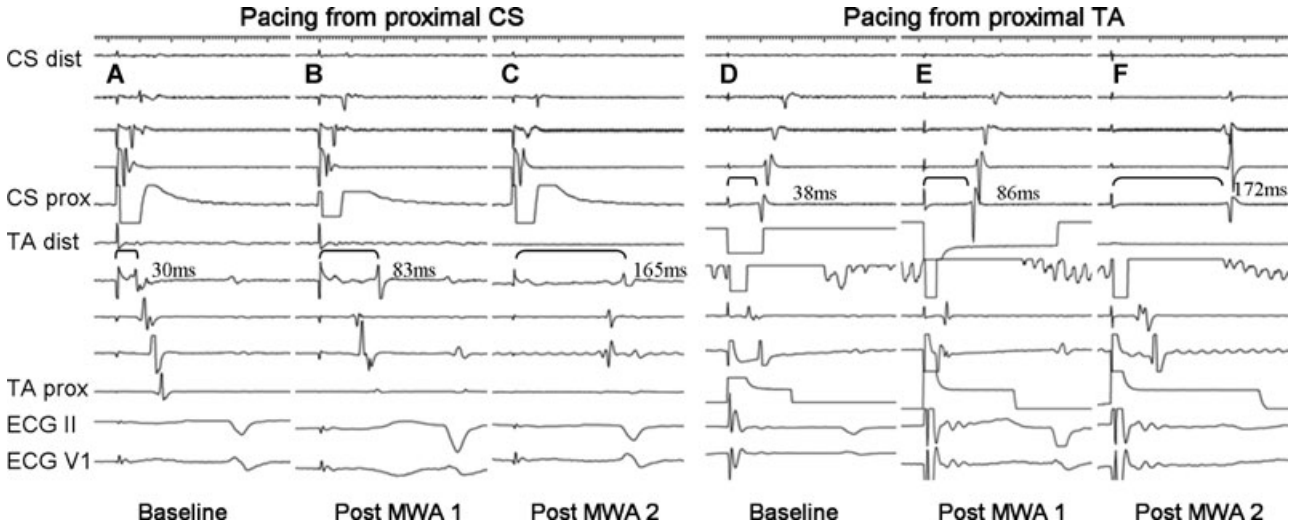

Figure 5. *Bidirectional block across the cavotricuspid isthmus (CTI). These are intracardiac and surface electrograms obtained during microwave (MW) ablation. The decapolar coronary sinus (CS) and tricuspid annulus (TA) catheters are represented as 5 bipolar electrograms arranged from distal (dist) to proximal (prox). The TA catheter was placed with the distal electrodes closest to the isthmus and the more proximal electrodes anticlockwise around the TA (It was impossible to satisfactorily pace or record from the most distal electrode pair and hence the next most distal pair was used instead). Before ablation, counterclockwise atrial flutter* (AFL) *(cycle length 185 ms) was inducible and conduction times across the isthmus (between the proximal CS and distal TA) were short (A and D). After the first MW ablation (MWA), the conduction time increased (B and E), but counterclockwise AFL, albeit with a slower cycle length of 197 ms, was still inducible. A further ablation resulted in even longer conduction times (C and F) and AFL was no longer inducible.*

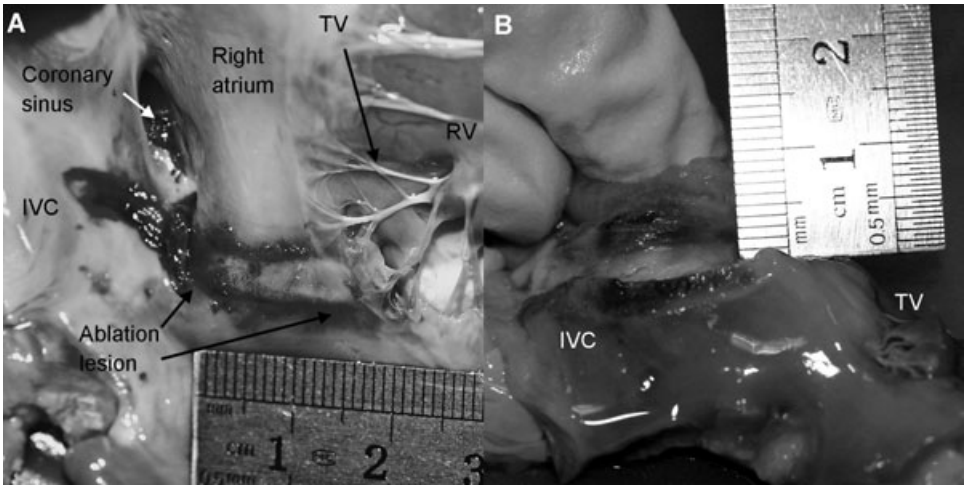

Figure 6. *Postmortem photographs of acute microwave (MW) ablation lesion. Panel A: Full length of ablation lesion immediately after ablation. Panel B: The lesion has been sliced open in its midline along its length to show transmurality of the lesion. IVC = inferior vena cava; RV = right ventricle; TV = tricuspid valve.*

At procedure 2, right AFL was still inducible in all 11 animals. Both clockwise AFLs (n = 9, cycle length 180 ± 13 ms) and anticlockwise flutters (n = 6, 180 ± 12 ms) were observed. AFL cycle lengths were not significantly different compared to those observed at the procedure 1 for clockwise flutters (P = 0.07) or anticlockwise flutters (P = 0.84).

MW Ablation

After 4.3 ± 3.3 ablations (range: 1–10, mean ablation time 131 ± 98 seconds), AFL was no longer inducible in all 11 sheep. Mean reflected power during the ablations was 4.0 ± 1.8 W (4.0 ± 1.8%). Local electrograms that were previously present in the CTI were no longer detectable following successful ablation. Conduction time from the proximal coronary sinus to lateral RA increased from 51 ± 14 ms to 118 ± 31 ms (P < 0.001) and also increased from 60 ± 13 ms to 119 ± 28 ms in the opposite direction (P < 0.001) (Fig. 5). There was usually a large increase in the conduction times after the ablation that rendered the AFL noninducible and reversed the activation direction in the lateral RA during coronary sinus pacing consistent with conduction block in the CTI. This was 55 ± 30 ms (range: 14–124 ms) from the proximal coronary sinus to the lateral RA (anticlockwise) and 52 ± 26 ms (range: 12–101 ms) from the lateral RA to the proximal coronary sinus (clockwise) and was significantly greater than the change in conduction times following ablations that did not abolish AFL inducibility (4 ± 13 ms [range: −17–55] and 2 ± 9 ms [range: −11–34], respectively, P < 0.001 for both). In 2 cases, an increase in bidirectional conduction time from the coronary sinus to the lateral RA and reversal of the activation pattern in the lateral RA was noted after an ablation, but AFL was still inducible though with a longer cycle length (Fig. 5). The activation sequence in the coronary sinus and tricuspid annulus catheters were unchanged and activation maps of these flutters showed that they were still right AFLs that were anticlockwise around the tricuspid annulus. A further ablation in both instances resulted in even more delayed activation in the lateral RA and noninducibility of the AFL. Activation maps of the cavotricuspid region during proximal coronary sinus pacing demonstrated that MW ablation was successful at creating a line of block in the isthmus (Fig. 2B) and that activation of the lateral RA was now via a longer path up the interatrial septum and over the right atrial roof.

We noted during the first few experiments that when the MW catheter was placed too medially, the MW catheter was positioned over the coronary sinus ostium that had prominent ridges at its anterior and posterior margins. As a result, the catheter was lifted off the inferior margin of the coronary sinus ostium and this region was not effectively ablated. In later experiments, we positioned the MW catheter more laterally to avoid these ridges (Fig. 4B). As a result, significantly fewer MW applications (2.2 ± 1.5 vs 5.8 ± 3.0, P = 0.03) and shorter ablation times (67 ± 47 seconds vs 175 ± 89 seconds, P = 0.03) were needed to reach the endpoint in the last 6 animals compared to the first 5. Among the last 6 animals, 3 required only a single ablation.

At autopsy, ablation lesions were seen in the target region but not elsewhere in the heart (Fig. 6). The average length of the MW ablation lesion was 24.3 ± 8.7 mm, average width was 8.8 ± 4.3 mm and average depth was 2.9 ± 0.4 mm. On macroscopic examination, all ablation lesions were transmural and hence the depth of the lesion was identical to myocardial thickness at the CTI. Epicardial fat was not affected by MW ablation macroscopically. These findings were also confirmed on histology. Thrombus that was adherent to the ablated region was seen in 3 sheep, but no charring was seen in any animals. The thrombus was adherent to the entire length of the macroscopically evident ablation lesion and was about 1–2 mm thick. The endocardium underlying the adherent thrombus was intact both on gross and histological examination. In 4 sheep, a small region of hyperemia was noted in a lobe of lung that lies between the caudal aspect of the heart and the diaphragm, in close apposition to the junction of the inferior vena cava and the RA.

Discussion

Our study provides proof of concept that it is possible to create electrically isolating linear lesions using a coaxial ring

slot array antennae in vivo using purely percutaneous techniques. By utilizing higher power ablations, we have been able to achieve bidirectional block of the CTI within practical ablation durations. The use of arrhythmia inducibility as the electrophysiological endpoint in an AFL ovine model is also closely analogous to the eventual clinical usage of MW ablation and provides a rigorous means to determine the efficacy of ablations.

MW Ablation

Percutaneous MW ablation catheters have been studied previously as an alternative energy source for the treatment of cardiac arrhythmias, but its percutaneous application has been limited by the long ablation times required. In canine model studies, between 160 and 312 seconds of ablation at 45–75 W was required to achieve block across the CTI.[12,13] When used in a clinical study, a similar catheter required 27.4 $\pm$ 14.7 ablations at 18 to 21 W for 120 seconds to achieve bidirectional block of the CTI.[11] However, the antennae design used in these studies were different to the ring slot array design used in this study. The high efficiency of our antennae design enables us to use much higher power outputs without resulting in high reflected powers and excessive heating of the coaxial cable. As a result, we were able to achieve bidirectional block with much shorter applications toward the end of our series of experiments. We needed a higher number of applications in the first 5 animals, which was most likely due to unfamiliarity with the handling and positioning of the catheter. Once we recognized that we had been positioning the MW catheter too medially and modified our technique by positioning the catheter more laterally and away from the septum (Fig. 4), we needed only 67 $\pm$ 47 seconds of ablations to achieve bidirectional block and noninducibility of AFL in the last 6 animals. In 3 of these sheep, a single 30-second application was sufficient. We avoided using excessive pressure when positioning the catheter but attempted to obtain uniform contact with the CTI along the length of the catheter.

Earlier ex vivo experiments have shown that the MW antenna array used in this study generates an even temperature distribution plot and is able to create long linear lesions in ex vivo myocardium 2.9 to 7.7 mm deep and 3.6 to 10.9 mm wide at various power levels.[17] In those ex vivo studies, the electric field was concentric around the long axis of the antenna and was even along the length of the antenna array and generated an elongated zone of hyperthermia (Fig. 3). In this study, we chose to use a high-power setting as we aimed to rapidly generate a transmural lesion. The rate of lesion formation has been a shortcoming of MW ablation in the past and part of the rationale for designing the ring slot array antenna was its ability to emit higher power outputs efficiently.[11,18] At this high-power setting, we were able to generate transmural lesions in an ovine model to create an electrically intact line of ablation but with minimal damage to surrounding tissue.

The ability to create deep lesions has its attendant risk of damaging surrounding tissues. We did not observe consistent significant damage to surrounding organs, but the effect of MW ablation on epicardial vessels remains unclear as the right coronary artery in sheep are small and nondominant and we could not confidently identify any epicardial vessels both macroscopically or microscopically in the vicinity of the ablation site.[19] This issue will require further study.

The sheep we used in this study weighed 48.6 $\pm$ 4.7 kg and hence were about 30% smaller than the average adult human. Their hearts were also smaller, as mammalian hearts are about 0.59% of body weight across all species.[20] This is a significant difference, but not one that is large enough to preclude the use of most equipment designed for human use in sheep. However, the range of human adult sizes varies greatly, with only below average weight adults similar in size to the sheep we used in this study. The implications of this size discrepancy are unclear and will require further study.

AFL Model

The ovine AFL model used in this study is closely analogous to CTI AFL seen in humans. In human AFL, activation proceeds around the tricuspid annulus, which forms the anterior boundary, while functional block in the crista terminalis forms the posterior boundary.[21] In this model, the tricuspid annulus similarly forms the anterior border while the posterior boundary is the intercaval line of ablation lesions.

In our study, we used not only evidence of bidirectional block as an endpoint, but also the abolition of arrhythmia inducibility to verify that we have created a line of block in the CTI. In most instances, this occurs simultaneously. However, we noted in 2 sheep that anticlockwise tricuspid annular AFL, which was confirmed on activation mapping, was still inducible despite bidirectional conduction delays that were consistent with conduction block and anticlockwise activation of the tricuspid annulus during proximal coronary sinus pacing. The authors believe that the most likely explanation is that there was persisting but slower conduction through the ablated region that was so delayed that activation of the lateral RA was still reversed during coronary sinus pacing. However, the persistence of conduction allowed AFL to be still inducible. It is possible that the persisting AFL could have another mechanism. However, in both instances, a further ablation of the CTI delayed the activation in the lateral RA even further, rendering the AFL noninducible. The authors thus concluded that it was most likely that the persisting AFL was CTI dependent in both these cases.

Residual slow conduction following ablation and the difficulty of ascertaining complete CTI block is well recognized in human studies, and differential pacing alone may not be adequate.[22,23] It may be that noninducibility of AFL as used in this study may be a more robust means of determining if there is conduction block across the line of ablation than just an increase in conduction times across it as has been used in previous studies.[12,13,24] As such, our ovine model of AFL may be a more rigorous means to test ablation technologies such as MW ablation than animal models with no inducible arrhythmias.

Another advantage of our animal model is that it is created entirely percutaneously, with no need for a thoracotomy. This is in contrast to previously described AFL models that relied on crush or incisional lesions in the RA to create an anatomical barrier.[15,16] This minimally invasive technique reduces the complexity of the procedure, reduces the distress for the study animals and facilitates postprocedural recovery. The use of the 3D mapping system allows the operator to ablate a continuous line of lesions reliably and reduces the difficulty of the procedure for the operator.

Conclusion

MW ablation using a ring slot array antennae can efficiently and rapidly create continuous and electrically intact linear lesions in a chronic ovine AFL model. The use of an animal model with an inducible arrhythmia allows us to demonstrate clearly that the MW ablation catheter can successfully ablate isthmus structures that are critical for sustained arrhythmia.

References

1. Borggrefe M, Budde T, Podczeck A, Breithardt G: High frequency alternating current ablation of an accessory pathway in humans. J Am Coll Cardiol 1987;10:576-582.
2. Nakagawa H, Jackman WM: Catheter ablation of paroxysmal supraventricular tachycardia. Circulation 2007;116:2465-2478.
3. McRury ID, Haines DE: Ablation for the treatment of arrhythmias. Proc IEEE 1996;84:404-416.
4. Rappaport C: Cardiac tissue ablation with catheter-based microwave heating. Int J Hyperthermia 2004;20:769-780.
5. Dorwarth U, Fiek M, Remp T, Reithmann C, Dugas M, Steinbeck G, Hoffmann E: Radiofrequency catheter ablation: Different cooled and noncooled electrode systems induce specific lesion geometries and adverse effects profiles. Pacing Clin Electrophysiol 2003;26:1438-1445.
6. Wittkampf FH, Nakagawa H: RF catheter ablation: Lessons on lesions. Pacing Clin Electrophysiol 2006;29:1285-1297.
7. Whayne J, Nath S, Haines D: Microwave catheter ablation of myocardium *in vitro*. Assessment of the characteristics of tissue heating and injury. Circulation 1994;89:2390-2395.
8. Knaut M, Tugtekin SM, Jung F, Matschke K: Microwave ablation for the surgical treatment of permanent atrial fibrillation–a single centre experience. Eur J Cardiothorac Surg 2004;26:742-746.
9. Knaut M, Spitzer SG, Karolyi L, Ebert HH, Richter P, Tugtekin SM, Schuler S: Intraoperative microwave ablation for curative treatment of atrial fibrillation in open heart surgery–the MICRO-STAF and MICRO-PASS pilot trial. MICROwave application in surgical treatment of atrial fibrillation. MICROwave application for the treatment of atrial fibrillation in bypass-surgery. Thorac Cardiovasc Surg 1999;47(Suppl 3):379-384.
10. Adragão P, Parreira L, Morgado F, Bonhorst D, Seabra-Gomes R: Microwave ablation of atrial flutter. Pacing Clin Electrophysiol 1999;22:1692-1695.
11. Chan JY, Fung JW, Yu CM, Feld GK: Preliminary results with percutaneous transcatheter microwave ablation of typical atrial flutter. J Cardiovasc Electrophysiol 2007;18:286-289.
12. Liem LB, Mead RH: Microwave linear ablation of the isthmus between the inferior vena cava and tricuspid annulus. Pacing Clin Electrophysiol 1998;21:2079-2086.
13. Iwasa A, Storey J, Yao B, Liem LB, Feld GK: Efficacy of a microwave antenna for ablation of the tricuspid valve-inferior vena cava isthmus in dogs as a treatment for type 1 atrial flutter. J Interv Card Electrophysiol 2004;V10;191-198.
14. Rosenblueth A, RamosJG: Studies on flutter and fibrillation: II. The influence of artificial obstacles on experimental auricular flutter. Am Heart J 1947;33:677-684.
15. Inoue H, Matsuo H, Takayanagi K, Murao S: Clinical and experimental studies of the effects of atrial extrastimulation and rapid pacing on atrial flutter cycle: Evidence of macro-reentry with an excitable gap. Am J Cardiol 1981;48:623-631.
16. Frame L, Page R, Hoffman B: Atrial reentry around an anatomic barrier with a partially refractory excitable gap. A canine model of atrial flutter. Circ Res 1986;58:495-511.
17. Chiu HM, Mohan AS: Computer aided design of miniaturized antennas for microwave cardiac ablation. In *Microwave Conference, 2001. APMC 2001. 2001 Asia-Pacific Microwave Conference, 2001. APMC 2001. 2001 Asia-Pacific Vol. 3*, 2001, pp. 1299-1302.
18. Yiu KH, Siu CW, Lau CP, Lee KL, Tse HF: Transvenous catheter-based microwave ablation for atrial flutter. Heart Rhythm 2007;4:221-223.
19. Frink RJ, Merrick B: The sheep heart: Coronary and conduction system anatomy with special reference to the presence of an os cordis. Anat Rec 1974;179:189-199.
20. Schmidt-Nielsen K. Circulation. In *Animal Physiology, Adaptations and Environment*, 5th ed. Cambridge: Cambridge University Press, 1997, pp. 91-123.
21. Olgin JE, Kalman JM, Fitzpatrick AP, Lesh MD: Role of right atrial endocardial structures as barriers to conduction during human type I atrial flutter: Activation and entrainment mapping guided by intracardiac echocardiography. Circulation 1995;92:1839-1848.
22. Friedman PA, Luria D, Munger TM, Jahangir A, Shen WK, Rea RF, Grice S, Asirvatham S, Packer DL, Hammill SC: Progressive isthmus delay during atrial flutter ablation: The critical importance of isthmus spanning electrodes for distinguishing pseudoblock from block. Pacing Clin Electrophysiol 2002;25:308-315.
23. Anselme F, Savoure A, Cribier A, Saoudi N: Catheter ablation of typical atrial flutter: A randomized comparison of 2 methods for determining complete bidirectional isthmus block. Circulation 2001;103:1434-1439.
24. Karolyi L, Spitzer SG, Geller L, Kiss O, Laszik A, Sotonyi P, Merkely B: Isthmus ablation with a novel microwave catheter in dogs. Eng Med Biol Mag, IEEE 2005;24:45-50.
25. Thavapalachandran S, Barry MA, Lim TW, Byth K, Ross D, Kovoor P, Thiagalingam A: Thermochromic myocardial phantom provides high spatial and temporal resolution of RF ablations. Heart Lung Circ 2008;17:S7.

This document is a scanned copy of a printed document. No warranty is given about the accuracy of the copy. Users should refer to the original published version of the material.